DEVELOPMENT OF A TUBE RECEIVER FOR A SOLAR-HYBRID MICROTURBINE SYSTEM

L. Amsbeck, R. Buck, P. Heller, J. Jedamski, R. Uhlig

German Aerospace Center (DLR), Institute of Technical Thermodynamics,

Pfaffenwaldring 38-40, D-70569 Stuttgart, Germany

Keywords: Solar gas turbine, solar tower plant, pressurized air receiver, tube receiver, hybrid, microturbine

Abstract

Solar-hybrid microturbine systems with cogeneration offer new possibilities for the generation of electricity and heat or air conditioning. The solar receiver is an important component of such a system. For a prototype system demo project a tube receiver for a 100kWe microturbine system is currently under development. The receiver is designed for air preheating up to 800°C at a pressure of 4.5 bar$_{abs}$. The challenge of the design is to find the right compromise between high efficiency, low pressure drop, high durability and low cost.

The receiver consists of multiple metallic tubes, arranged in a cavity and connected in parallel. For the design the knowledge of local flux density, fluid and material temperature is required. A finite-element program coupled with a ray tracer was used for the layout.

The final receiver design is described, which was optimized with respect to efficiency, material temperatures and pressure drop. Expected performance data for nominal load and off-design conditions will be presented, including the expected annual receiver and system performance. In addition, several possibilities for future improvements will be outlined.

1   Introduction

Worldwide growth of energy demand, the expected peak of oil production, the search for supply security and fossil-fuel based climate change result in the actual development of several renewable energy technologies. After wind technology is gaining significant world electricity market share yet the same is hoped for solar based systems. For the solar source photovoltaic, concentrating photovoltaic and concentrating solar thermal systems are promising options for the large scale electricity market. A major component of a price competition in the future will be the capability of the whole electricity system to follow the electricity demand. Fluctuating sources like the sun need storage, back-up power plants or hybrid operation, if a large electricity market share should be reached. For PV a wide use of plug-in electric vehicles in the future could provide a battery capacity, but the costs and losses of such a storage system will not be negligible as batteries are expensive and limited in the number of load cycles.

In contrast to PV solar thermal power systems with heat storage or hybrid operation offer a non-fluctuating power source at low costs with no need of electric storage or back-up plants. A hybrid operation with biomass-based fuel can also be nearly CO_2-neutral. As low cost high temperature heat storage needs some more development and solar only systems are limited in maximum operation temperatures and therefore in efficiency hybrid systems seem to be the better configuration, at the cost of dependence on biomass-based fuel for CO_2-neutral power. With the allowance of 50% biomass co-firing in the actual Spanish Royal Decree 661/2007 economic opportunities for such concepts exist.

A demonstration project with a test unit at a power level of 230 kW$_{el}$ showed already the feasibility of solar-hybrid gas turbine systems[1] . System studies predict attractive electricity cost for the solar fraction, as low as about 0.08 € /kWh[2]. Due to the risk with the implementation of new technologies, the first commercial plants are likely to be built at small power levels, for example, as cogeneration plants[3].

The paper describes the development of an important component of such a system, the receiver.

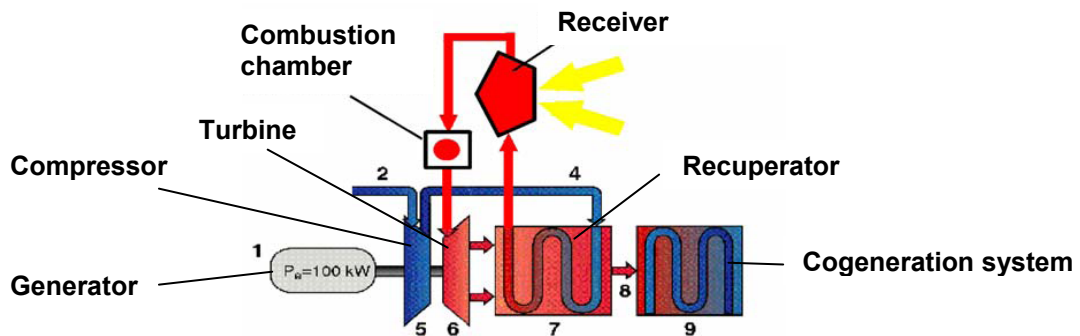## 2   System description and design targets

**Figure 1: Flow scheme of the microturbine system
with a solar receiver and cogeneration**

Within the SOLHYCO project, (co-funded by the EC under Contract No. 19830), a solar-hybrid microturbine system is under development and will be tested in 2008. The microturbine is a TURBEC T100 model with 100 kW_e nominal power and a turbine inlet temperature at design point of around 950°C at a mass flow of 0.8 kg/s and 4.5 bar_{abs}. The microturbine shows in the unmodified natural gas mode an efficiency of 31%[4]. The receiver is placed between the recuperator and the combustion chamber as seen in Figure 1. With a recuperator outlet temperature of 600°C at design point and an air preheating up to 800°C the receiver delivers a thermal power of 181.9kW.

For the SOLHYCO project it was decided to develop a metallic tube receiver instead of using the available volumetric receiver technology to reduce costs for the receiver and the security measures. The challenge of the design was to find the right compromise between high efficiency, low pressure drop, high durability and low cost.
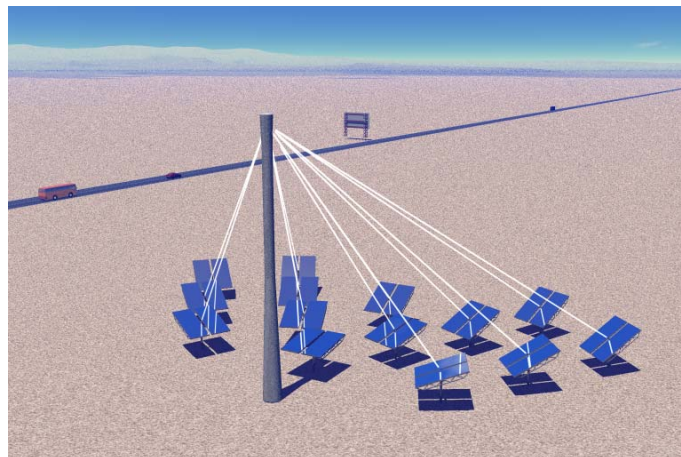

Figure 2: Solar microtower plant

Figure 2 shows the reference heliostat field for which the receiver is developed. It consists of 13 heliostats of 25 m² each canted for the 21.11. 12.00. The tower height is 24 m, the receiver angle against the horizon is about 46° and the design location is Seville, Spain (37.2° latitude).

Receiver design targets are:
- efficiency: as high as possible
- maximum tube temperature for nickel-based alloys: 900°C
- simple distributor and collector
- layouts limited to straight tubes to allow later the application of parallel developed multi-layer tubes for higher outlet temperatures
- pressure drop: as low as possible, maximum 100 mbar (ensured surge limit of the compressor)

A maximum tube temperature is not a fully sufficient criterion to reach a reasonable lifetime, but an exact lifetime analysis considering load cycles, creep and fatigue was not possible in the work yet.

3   Heat transfer enhancement

Reflection of solar radiation, heat conduction through the cavity walls and convection plus thermal radiation through the aperture are the loss mechanisms of solar receivers. For tube receivers to heat air for a microturbine the thermal radiation is the dominating loss mechanism. The smallest thermodynamically possible loss is given by the in- and outlet temperature of the air. Higher losses are mainly affected by the temperature difference between the tube outer wall and the fluid, the driving temperature difference to bring the absorbed solar radiation into the fluid. With air as the working fluid this temperature difference is dominated by the heat transfer, the heat resistance of the wall is much smaller.

To achieve a smaller driving temperature difference there are two possibilities: enlargement of the heat transfer area or heat transfer enhancement. Enlargement of the heat transfer area results in a proportional increase of costs for the absorber tubes if the diameter is kept constant. The total tube length has a big influence on the overall costs, especially with the sharp increase in nickel price over the last years, but also on the efficiency. As the overall costs were not known at the beginning of the project an optimisation was not possible and therefore the total tube length was set to 100m for an available 26.7mm x 2.11mm (outer diameter x wall thickness) tube. If tubes with smaller diameter and smaller wall thickness would be available, the same heat transfer area could be provided with less material and the same stress security factor. But for normal available cold drawn tubes the lower limit of wall thickness is about 1.5mm. Thus the biggest diameter with a sufficient stress security factor leads to the lowest price of heat transfer area.

Heat transfer enhancement can be the much cheaper possibility. For the choice of an enhancement for the tube receiver the first criterion is the ability of manufacturing as no stock source of enhanced high temperature tubes is known to the authors. The performance of the enhancement is the second criterion. The heat transfer can be enhanced by three main mechanisms: First, higher fluid velocities and therefore higher heat transfer coefficients can be achieved by inserts like twisted tape or for a given total tube length by connecting fewer tubes in parallel and by elongating the tubes. The limitation for this mechanism is given by the higher pressure drop which results from the higher fluid velocities. The second mechanism is the local enlargement of the heat transfer area by ribs, foams etc. This mechanism is limited by the heat conduction of the used material. The third mechanism is based on the destruction of the thermal boundary layer and a promoted mixing of heated air with the colder core of the flow. This disturbance can be achieved by ribs, convex or concave dimples, pins etc. The limitation for this mechanism is again a higher pressure drop. Most heat transfer enhancements use more than one mechanism. The most efficient measures are helically ribs, foams or dimples.
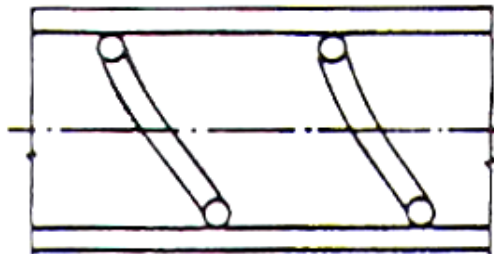

Figure 3: Wire-coil heat transfer enhancement

For the tube receiver a wire-coil insert[5] was chosen (see Figure 3), because it is easily applicable to every tube and shows a reasonable enhancement. It destroys the thermal boundary layer and mixes the fluid, but doesn't introduce much new areas which don't contribute to the heat transfer, but contribute to the pressure loss. The heat transfer area is not enlarged, as the thermal contact between wire and wall is low.

4   Pre-dimensioning

To achieve the smallest driving temperature difference ΔT the number of tubes n, the diameter of the wire e and the axial pitch of the wire-coil p are optimised. This means to maximise the heat transfer coefficient for the given total tube length $n \cdot l$, the maximum pressure drop Δp, the inner tube diameter d and the nominal heat flux $\dot{Q}$. The pressure drop was set to 70mbar in the absorber tubes to allow another 30mbar pressure drop in the connection pipes.

Aim function to minimize:
$$\Delta T = \frac{\dot{Q}}{n \cdot d \cdot l \cdot \pi \cdot \dfrac{Nu \cdot \lambda}{d}}$$

Definitions:

$$Nu = 0.253 \cdot \mathrm{Re}^{0.716} \cdot \left(\frac{e}{d}\right)^{0.372} \cdot \left(\frac{p}{d}\right)^{-0.171}$$

$$f = 5.153 \cdot \log(\mathrm{Re})^{-1.08} \cdot \left(\frac{e}{d}\right)^{0.796} \cdot \left(\frac{p}{d}\right)^{-0.707} \qquad \Delta p = f \cdot \frac{l}{d} \cdot \frac{\rho}{2} \cdot \left(\frac{4 \cdot \dot{m}}{n \cdot d^2 \cdot \pi \cdot \rho}\right)^2$$

Side conditions:
$$0.35 \le \frac{p}{d} \le 2.48 \qquad 0.037 \le \frac{e}{d} \le 0.09 \qquad 15000 \le \mathrm{Re} \le 100000$$

$$\Delta p \le 7000 Pa \qquad n \cdot l = 100m \qquad d = 0.02248m$$

With fluid properties from the average temperature of 700°C and 4.5bar the optimisation results in:
$\Delta T = 67.1°C$ $n = 40$ $l = 2.5m$ $\mathrm{Re} = 26548$ $e = 2mm$ $p = 55.4mm$

A comparison to a normal tube (technical smooth) at optimum for the same tube length results in:
$\Delta T = 92.5°C$ $n = 26$ $l = 3.846m$ $\mathrm{Re} = 40843$.

Or for the same $\Delta T = 67.1°C$ the normal tube needs $n = 30$ $l = 5.16m$ $\mathrm{Re} = 35397$ giving a total tube length of 154.8m. This comparisons show the benefit of the wire-coil insert, a reduction of the driving temperature difference by 25.4°C or 27.5% or a reduction of the total tube length of 54.8m or 35.4%.

5   Modeling

5.1   3D-simulation model

To enable an exact simulation of the receiver a 3D-finite-element (FE) model was created. This model uses shell elements for the thermal calculations to achieve short computation times. Only the absorber tubes and the cavity are considered in the model, distributor and collector are neglected. For the simulation of the solar radiation distribution and the reflection loss an extension was introduced into the solar tower simulation tool MIRVAL. This extension allows the ray tracer to evaluate fluxes on the FE-mesh elements. The thermal behaviour of the fluid in the tubes is considered using Nusselt–correlations for the heat transfer and by simulating the heat transport of the fluid. The exchange of thermal radiation between tubes, walls and environment is included assuming an emissivity of 0.9 for the tube in the solar and the thermal wavelength range. For the cavity wall the emissivity for the solar range is set to 0.1 and for the thermal range to 0.5. Reflection and emission are assumed to be completely diffuse.

By now, convection losses through the aperture are not considered and the cavity is assumed to be adiabatic. Furthermore the mass flow is assumed to be the same in every tube.

From the solution, the temperature field, all relevant thermal values like efficiency, maximum tube temperature, tube outlet temperature distribution and pressure losses are calculated. The temperature field will later be used for a more detailed lifetime analysis.

5.2   Annual performance model

To analyse the annual receiver performance 3D-FE runs for different time points according to the following scheme were conducted: Time points are set at every full hour plus further points at dawn and dusk at the 21st of every month. The symmetry of the sun positions over the day like 10.00 to 14.00 and over the month like April to August is used to reduce the number of time points. The overall time point number is 50. For the Direct Normal Insolation (DNI) the Hottel model[6] is used. The annual yield is finally corrected with a measured DNI. The aperture diameter was optimized to achieve the highest possible annual yield. If the receiver is loosing power due to too low intercepted power which happens for a short time after dawn and before dusk, the receiver is not operated.

For the system performance full power operation whenever there is enough sun and 4000 full load hours per year are assumed. Gas turbine system efficiency is 28% due to the inclusion of the receiver, compared to 31% in the conventional system.

6 Results and Discussion
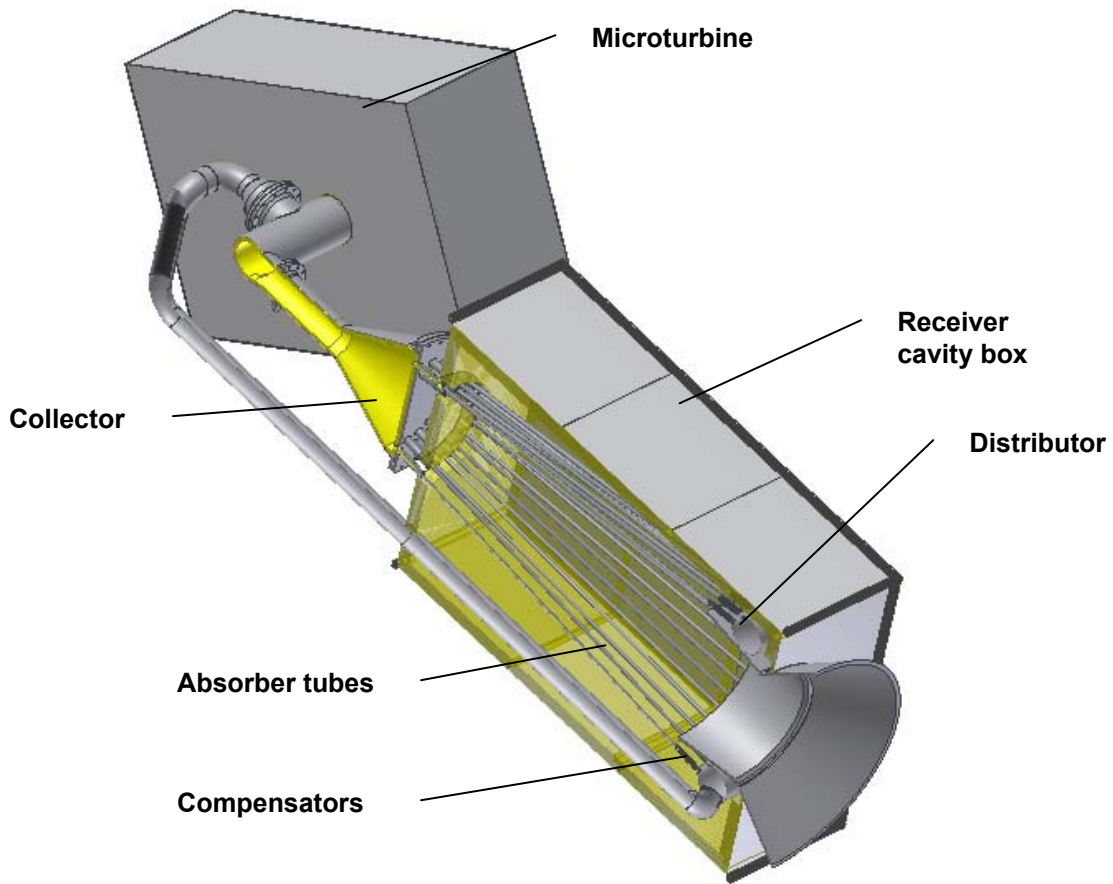
6.1 Receiver design

Figure 4: Half-section of the SOLHYCO-receiver with cavity and microturbine

The SOLHYCO-receiver consists of 40 absorber tubes, each 2.5m long, made of the nickel based superalloy Inconel 600, arranged in a cavity and connected in parallel. The aperture diameter is 0.9m. The absorber tubes are mounted on one radius at the distributor and on two radii on the collector (see Figure 4) forming a cone-like absorber geometry. The distributor in form of a torus is made of tube bends, the collector is made of a flat lid flanged onto a reduction cone. The distributor is made of a heat resistant 12%-chrome steel. The collector is insulated from the inside to avoid the need of thick walled structures of high temperature alloy which are very costly. It also uses the 12%-chrome steel. Internally insulated pipe pieces are used for the connection of the absorber tubes with the collector. Together with a minimum distance between the tubes needed for welding the minimum collector radius is defined.

Every absorber tube is equipped with one compensator at the connection between distributor and absorber tubes to allow different thermal expansion. Spring hangers are used for a flexible suspension.
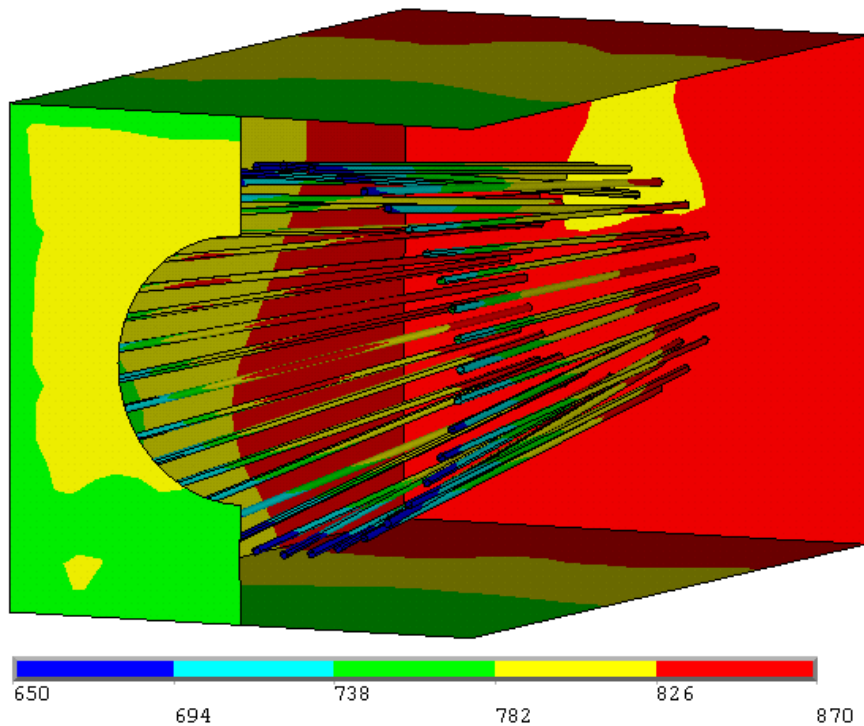
6.2 Receiver performance at design point

Figure 5: Outer wall tube and cavity temperatures at design point [°C] at a half opened cavity

Input power [kW]	234,6	Solar reflection loss [kW]	8,5
DNI [W]	850	Total thermal radiation loss [kW]	43,1
Aperture diameter [m]	0,9	Thermal radiation loss from the absorber tubes[kW]	13,7
Delivered Power [kW]	182,2	Thermal radiation loss from the cavity walls [kW]	29,4
Efficiency [%]	77,7	Outlet temperature [°C]	800

Table 1: Performance data of the receiver at design point

The maximum tube temperature at design point (21.3) of 867°C as seen in Figure 5 does not exceed the 900°C target temperature. Therefore the design fulfils the targets at design point. The cone shape of the tubes results in the highest absorbed solar fluxes at the beginning of the tubes. Together with the inlet for the cold air at the base of the cone relatively low maximum tube temperatures are achieved.

The efficiency at design point of 77.7% is low compared to a volumetric receiver, due to the small heat transfer area compared with the volumetric receiver. A smaller aperture would result in a better design point performance even with included field efficiency, but the aperture diameter is deduced from an optimisation of the annual yield, where the bigger aperture reduces the spillage losses.

Table 1 shows that the absorber tubes contribute only with 13.7kW to the total thermal radiation loss of 43.1kW (32%). Smaller gaps between the tubes would raise this share and enhance the efficiency, as only the tube surface temperature contributes to the heat flux into the fluid. Furthermore the solar reflection loss would be lower. A further reduction of the gaps was not possible for this design due to the optimised number and length of tubes and due to limits from manufacturing.

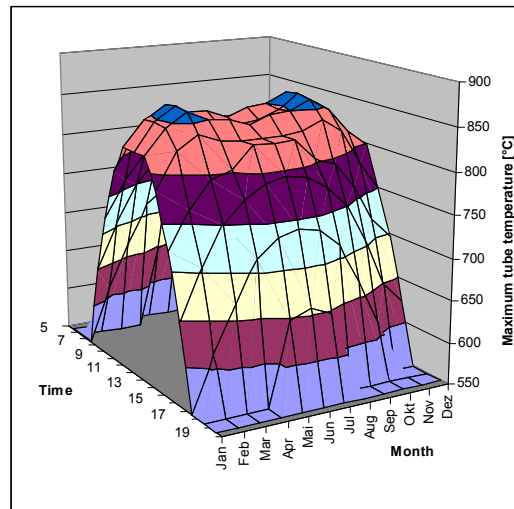### 6.3 Receiver off-design performance

Figure 6: Maximum tube temperatures [°C] over the year

Figure 6 shows the variation of the maximum tube temperature over the year. As the tube temperature never exceeds 900°C the design fulfils the targets. Again the cone shape contributes to this robust behaviour. At off-design points the radiation over the cone circumference is much more inhomogeneous with higher peaks. But the lower input power compared to the design point together with the low fluid temperatures at the cone base, where the peaks occur, lead to good off-design performance.

The robust behaviour is believed to not require an active control of the maximum tube temperatures in a commercial product. Nevertheless in the test receiver an active control for some high-loaded tubes is foreseen, due to uncertainties from the heliostat field. This active control will consist of a tube outlet temperature measurement and mixing of the tube inlet flow with colder air from a branch before the recuperator. System simulations showed a low impact of this measure onto the system efficiency. A further advantage of this concept is the avoidance of 600°C valves.

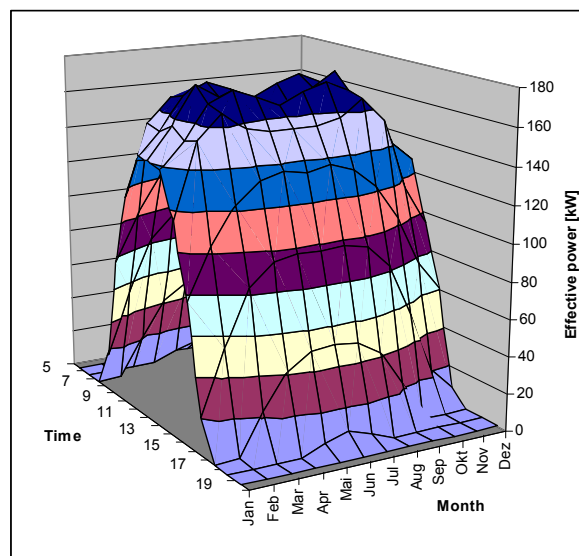### 6.4 Annual receiver performance

Figure 7: Effective power [kW] over the year

Figure 7 shows the effective power over the year. With a correction of the annual DNI from the Hottel-model of 2612 kWh/m^{2}a with a measured DNI of 2015kWh/m^{2}a the integrated yield is 330 MWh$_{th.}$. With a corrected intercepted power of 447 MWh$_{th}$ this results in an average efficiency of the receiver of 73.8% at a heliostat field efficiency of 68.3%. The receiver efficiency is rather low and the heliostat field efficiency is rather high, which results from the big, but optimised aperture diameter for the chosen canting point.

With an efficiency of 28% and 4000 full load hours the microturbine needs a thermal energy input of 1429 MWh$_{th.}$. As 330 MWh$_{th.}$ are contributed by the receiver, the solar share reaches 23.1%. The low solar share is due to the low outlet temperature of the receiver.

7 Future improvements

To improve the efficiency of the receiver a quartz window will be later implemented to reduce thermal radiation and convection losses. This window was already manufactured and is coated with a high temperature antireflective coating to reduce the solar reflection losses introduced by the window.

A further improvement is to adapt the mass flow through the absorber tubes by passive measures. At the test receiver pressure loss elements can be used on the tubes with low loads to increase the mass flow through the high loaded tubes. In a commercial receiver this pressure drop elements can be substituted by heat transfer enhancements with different pressure loss for different tubes, giving again a slight improvement of performance. A reasonable increase of the solar share could be reached with an increase of the receiver outlet temperature to 900°C. But this can only be reached with a much larger heat transfer area to reduce the maximum temperature. Another option is the development of profiled multilayer tubes, which is done in parallel.

8 Summary

The design of a receiver for a solar-hybrid microturbine system is described. The receiver consists of multiple metallic tubes, arranged in a cavity. After the selection of an appropriate heat transfer enhancement, a pre-dimensioning of the absorber tubes was made, assuming a total tube length of 100m. A cone shape layout was evaluated in detail at design and off-design conditions with a 3D-FE code coupled with a ray tracer. The results indicate robust receiver behaviour under all operation conditions. With an outlet temperature of 800°C the receiver reached an annual efficiency of 73.8%, neglecting the convection losses and the heliostat field at design location Seville, Spain reached an annual efficiency of 68.3%. Finally future improvements like an aperture window, mass flow adaption and a higher receiver outlet temperature are discussed.

References

[1] Heller, P., Pfänder, M., Denk, T., Tellez, F., Valverde, A., Fernandez, J., and Ring, A., 2006, "Test and valuation of a solar powered gas turbine system," Sol. Energy, **80**(10), pp. 1225–1230.

[2] Romero, M., Buck, R., Pacheco, J. E., 2002, "An update on solar central receiver systems projects and technologies," J. Sol. Energy Eng., 124, pp. 98–108.

[3] Romero, M., Marcos, M. J., Téllez, F., Blanco, M., Fernández, V., Baonza, F., and Berger, S., 1999, "Distributed power from solar tower systems: A MIUS approach," Sol. Energy, **67**(4–6), pp. 249–264.

[4] Turbec, "T100 microturbine system: technical description", company information brochure

[5] Zhang,Y.F.,Liang,Z.M., 1991,"Heat transfer in spiral-coil-inserted tubes and its application," in Advances in Heat Transfer Augmention, M.A. Ebadin, D.W. Pepper and T.Diller, Eds.,ASME Symp. Vol. HTD, **169**, 31-36.

[6] Hottel H. C., 1976, "A simple model for estimating the transmittance of direct solar radiation through clear atmospheres, " Solar Energy, .**18**, 129-134.